Inhomogeneous time-reversal symmetry breaking in Sr$_2$RuO$_4$

Roland Willa [ORCID],[1,*] Matthias Hecker [ORCID],[1] Rafael M. Fernandes,[2] and Jörg Schmalian[1,3]

[1]*Institute for Theory of Condensed Matter, Karlsruhe Institute of Technology, Karlsruhe 76131, Germany*
[2]*School of Physics and Astronomy, University of Minnesota, Minneapolis, 55455 Minnesota, USA*
[3]*Institute for Quantum Materials and Technologies, Karlsruhe Institute of Technology, Karlsruhe 76021, Germany*

We show that the observed time-reversal symmetry breaking (TRSB) of the superconducting state in Sr$_2$RuO$_4$ can be understood as originating from inhomogeneous strain fields near edge dislocations of the crystal. Specifically, we argue that, without strain inhomogeneities, Sr$_2$RuO$_4$ is a single-component, time-reversal symmetric superconductor, likely with $d_{x^2-y^2}$ symmetry. However, due to the strong strain inhomogeneities generated by dislocations, a slowly decaying subleading pairing state contributes to the condensate in significant portions of the sample. As it phase winds around the dislocation, time-reversal symmetry is locally broken. Global phase locking and TRSB occur at a sharp Ising transition that is not accompanied by a change of the single-particle gap and yields a very small heat capacity anomaly. Our model thus explains the puzzling absence of a measurable heat capacity anomaly at the TRSB transition in strained samples and the dilute nature of the time-reversal symmetry broken state probed by muon spin rotation experiments. We propose that plastic deformations of the material may be used to manipulate the onset of broken time-reversal symmetry.

I. INTRODUCTION

Establishing the symmetry of the Cooper pair wave function is the pivotal step to understand a superconductor. It not only determines the macroscopic phenomenology, but it also narrows down the microscopic mechanism of the pairing state. Arguably the strongest evidence that cuprate-based high-temperature superconductors are governed by an electronic mechanism is the observation of the $d_{x^2-y^2}$ symmetry of the pair wave function [1,2]. Sr$_2$RuO$_4$ is a layered perovskite superconductor that is isostructural to La$_2$CuO$_4$ [3]. Given the crossover from incoherent to coherent transport as a function of temperature, Sr$_2$RuO$_4$ is—just like the cuprates—governed by strong electronic correlations [4]. However, early on it was advocated that the more appropriate analog for the origin and symmetry of the pairing state might be ^{3}He [5,6]. Indeed, in distinction to the cuprates, broken time-reversal symmetry below T_c was observed in muon spin relaxation [7,8] and polar Kerr effect [9] measurements, reminiscent of the $p_x + ip_y$ pairing state of the A phase of ^{3}He.

Recently, several experiments have forced the community to reexamine widely accepted beliefs about this fascinating material. Nuclear magnetic resonance (NMR) measurements revealed that Sr$_2$RuO$_4$ is in fact a spin-singlet superconductor [10–12]. Applying uniaxial strain leads to a separate onset of superconductivity at T_c and of time-reversal symmetry breaking (TRSB) at T_{TRSB} [8]. Combined with the observed jump of certain elastic constants across T_c [13,14], these observations have led to the proposal that Sr$_2$RuO$_4$ is a two-component singlet superconductor, with T_{TRSB} signaling the condensation of the second component [15–20]. Meanwhile, there is no indication of a heat capacity anomaly at T_{TRSB} [21], in contrast

to the sharp jump seen at T_c. More generally, there is no experimental evidence that time-reversal symmetry breaking is a bulk effect—in fact, muon spin rotation (μSR) experiments find variations of the effect for distinct samples and
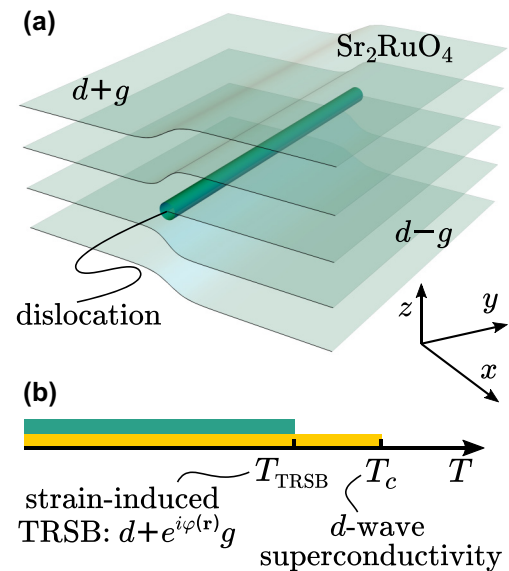

FIG. 1. (a) Edge dislocation in Sr$_2$RuO$_4$ inducing local breaking of time-reversal symmetry due to inhomogeneous strain. Near the dislocation, large strain fields mix a primary $d_{x^2-y^2}$ pairing state with other subleading symmetry channels, e.g. a $g_{xy(x^2-y^2)}$ pairing state [16]. As a result, $d \pm g$ pairing emerges on opposite sides of the dislocation, forcing the relative phase $\varphi(\boldsymbol{r})$ to wind in between, thus breaking time-reversal symmetry locally. (b) Time-reversal symmetry breaking appears in the bulk system as a stand-alone phase transition where the local phase windings are locked through the long-range decay of strain fields that couple dislocations.

*Corresponding author: roland.willa@kit.edu

signatures consistent with diluted magnetic moments [8]. This calls into question the widely accepted view that Sr_2RuO_4 is a multicomponent superconductor.

In this paper, we argue that the pairing states of Sr_2RuO_4 and the cuprate superconductors display significantly more parallels than previously thought. Specifically, we argue that Sr_2RuO_4 without strain inhomogeneities is a single-component, time-reversal symmetric superconductor with a $d_{x^2-y^2}$ pairing state. This is consistent with recent quasiparticle interference measurements [22] that strongly favor such a pairing state, despite the onset of TRSB. The recently discussed phase diagram of strained Sr_2RuO_4, where superconductivity occurs in the vicinity of a state with magnetic order, likely a spin-density wave [8], is also suspiciously similar to the generic cuprate phase diagram with a state of antiferromagnetic order vanishing near superconductivity.

In our theory, time-reversal symmetry breaking of Sr_2RuO_4 is a consequence of strong strain inhomogeneities that locally break the crystalline symmetry and, due to the large mechanical stresses, condense a subleading pairing state. We analyze the nucleation of the corresponding pairing wave function and its nontrivial phase windings near edge dislocations of the crystal. In particular, we solve for the pairing state near a single edge dislocation and proceed with a coarse-grained model of many such dislocations. The first part of the theory demonstrates that inhomogeneous strain induces local phase windings, see Fig. 1(a); the second shows the emergence of global phase locking. This yields a sharp phase transition where time-reversal symmetry is globally broken, see Fig. 1(b), albeit with a weak heat-capacity anomaly. It hence explains the absence of a calorimetric signature at T_{TRSB} in strained samples [21], which is strong evidence against any scenario where breaking of time-reversal symmetry is associated with the opening of a quasiparticle pairing gap.

Despite the similar pairing state, an important difference between Sr_2RuO_4 and the cuprates is that at least one other pairing state must be sufficiently close in energy to contribute to the condensate near strong local strain inhomogeneities. The idea that a second competing superconducting instability is likely present in this material was proposed before both on phenomenological and microscopic grounds [16–19,23]. In distinction to these investigations, the subleading instability of our theory does not need to be fine tuned to have approximately the same T_c value as that of the leading d-wave instability. Moreover, because the dislocation induces strain in all symmetry channels, TRSB occurs independently of the subleading state's symmetry—s wave or g wave. Finally, in our scenario, TRSB does not correspond to the homogeneous condensation of the second pairing state but to a collective phenomenon in which the phase windings of the subleading pairing wave function induced near a dislocation phase-lock globally. A direct consequence of the assumption of competing superconducting instabilities is that, in a clean sample, the subleading pairing state should lead to a Bardasis-Schrieffer excitation [24] in the electronic Raman spectrum. Finally, strain engineering of Sr_2RuO_4, e.g., via plastic deformation of the sample, which is known to impact dislocations in other perovskites [67], may be used to create and manipulate time-reversal symmetry broken superconducting states.

II. RESULTS

A. Overview of the experimental constraints on the pairing state

Before we present our theory we summarize some of the relevant experimental observations and their puzzling implications that motivated our proposal. Excluding accidental degeneracies, homogeneous TRSB at T_c may only occur for a superconducting order parameter that has at least two components, i.e., transforms according to a two- or higher-dimensional irreducible representation of the symmetry group [25]. For Sr_2RuO_4, with D_{4h} point group, this leaves only two options: E_u triplet pairing that transforms like $p_x \pm ip_y$ or the E_g singlet pairing of the type $d_{xz} \pm id_{yz}$. The most recent NMR measurements strongly favor singlet pairing [10–12]. Furthermore, μSR experiments under uniaxial stress report a clear splitting between the superconducting transition temperature T_c and the onset temperature for broken time-reversal symmetry, $T_{TRSB} < T_c$ [8]. For such a two-component order parameter, uniaxial stress should indeed lift the degeneracy. In this picture, the strain-favored component first condenses to a single-component state at T_c, while the strain-disfavored component mixes-in with relative phase $\pm\pi/2$ at T_{TRSB}. Numerous theories for Sr_2RuO_4 consider either $p_x \pm ip_y$ triplet pairing [5,6,26–29] or, given the recent NMR results of Refs. [10–12], $d_{xz} \pm id_{yz}$ singlet pairing [15,20,30].

There is, however, one very robust thermodynamic argument against either of these mean-field scenarios (see also Appendix A): Recent heat-capacity measurements in strained samples [21] see no jump at T_{TRSB} and a large discontinuity at T_c. Within mean-field theory, the ratio of the heat-capacity jumps at T_c and T_{TRSB} are generally related to the slopes $dT_c/d\epsilon_{B_{1g}}$ and $dT_{TRSB}/d\epsilon_{B_{1g}}$, see Ref. [8]. If the magnitudes of the slopes are assumed to be approximately equal for small strain, the heat-capacity jumps must essentially be the same. In the more realistic case, as determined by the experimental strain-temperature phase diagram, where $|dT_{TRSB}/d\epsilon_{B_{1g}}| < dT_c/d\epsilon_{B_{1g}}$, the jump at the lower transition must even be the largest one. This is in sharp contrast to the measurements of Ref. [21], which reports no anomaly at the lower transition temperature, estimating an upper bound for the second discontinuity at T_{TRSB} of less that 5% of the discontinuity $\Delta C(T_c)$ at T_c. This finding provides strong thermodynamic evidence against a BCS-type transition of either E_g or E_u symmetry. More generally, the absence of a heat-capacity jump at T_{TRSB} argues against any scenario where the opening of a pairing gap affects the entropy of electronic quasiparticles. In addition, the quadratic dependence of T_c with strain [31,32] and the absence of a jump in the elastic constant in the B_{1g} symmetry channel [13] constitute additional evidence against a two-component order parameter with E_g or E_u symmetry. For further discussions about the puzzles related to the chiral E_g or E_u pairing states, see Refs. [16,33–35].

Given this strong evidence against a symmetry-protected, two-component order parameter, the notion of an accidental (near) degeneracy of two single-component order parameters seems a very compelling approach [16–19,23]. This is rooted in significant microscopic evidence that electronic pairing mechanisms give rise to several competing superconducting states [17,23,36,37]. A range of arguments is brought forward in Ref. [16] supporting the degeneracy between $\psi_d = d_{x^2-y^2}$

and $\psi_g = g_{xy(x^2-y^2)}$ pairing. This state is further supported by the observed jump of the elastic constant in the B_{2g} symmetry channel [13,14], see also Ref. [38], and by the report of vertical line nodes [39]. Other candidates include the near degeneracy between $\psi_d = d_{x^2-y^2}$ and a nodal s-wave state ψ_s [17] or the degeneracy between singlet and triplet states in a model that focuses on the quasi-one-dimensional parts of the electronic structure [19]. Notice, an implication of the small heat-capacity signature at the lower transition is that the amplitude of this second component must be exceedingly small; see Appendix A.

That the primary pairing state is indeed unconventional is most plainly demonstrated by the system's strong sensitivity to nonmagnetic disorder [40,41]. It is further supported by thermal conductivity measurements [39], which report vertical nodal lines, and by the recent quasiparticle interference measurements of Ref. [22]. It is also in line with numerous microscopic theories for unconventional pairing in this compound [19,22,36,37,42–44]. Our approach—partially inspired by Ref. [16]—relies on the existence of a secondary order parameter that is reasonably close in energy and that admixes to the primary phase in the presence of inhomogeneous strain. However, in distinction to Ref. [16], we neither require an almost perfect degeneracy of both states for unstrained homogeneous samples, nor do we expect a second homogeneous mean-field-like transition anywhere below the onset of superconductivity at T_c. Instead, we argue that the breaking of time-reversal symmetry is exclusively a consequence of strain inhomogeneities in the material.

The presence of inhomogeneous strain fields was clearly established in scanning SQUID microscopy measurements on Sr$_2$RuO$_4$ single crystals [32]. The strong coupling of edge dislocations to superconductivity was revealed in Ref. [45], where the local superconducting transition temperature in the vicinity of a lattice dislocation can reach almost twice the value of the bulk. Finally, we note that there is really no evidence at this point that the TRSB transition in Sr$_2$RuO$_4$ is a mean-field homogeneous phase transition of the bulk system. This observation of TRSB in the unstrained or weakly strained sample—which we aim at explaining here—is qualitatively distinct from the appearance of a bulk spin-density wave order under large uniaxial stress (~1 GPa), i.e., when the system is driven through a Van Hove singularity. At low stresses, the μSR signal shows a broad distribution of local magnetic moments, somewhat similar to what is often observed in spin glasses [7,8]. In fact, the authors of Ref. [8] explicitly state that the internal field is thought to arise at edges, defects, and domain walls. In addition, the splitting of $T_c - T_{\text{TRSB}}$ determined in Ref. [8] varies in magnitude *and* sign between different samples. These observations guided us to investigate the role of inhomogeneous strain fields. We will first analyze the behavior in the vicinity of a single edge dislocation. In a second step we will formulate an effective model to describe the case of many dislocations.

B. Time-reversal symmetry breaking at a single dislocation

In what follows, we consider a Ginzburg-Landau theory for the superconducting order parameter $\psi = (\psi_d, \psi_g)$, where the two components belong to different one-dimensional irre-

ducible representations, i.e., they do not transform into each other under a crystalline symmetry. As discussed, we have in mind a primary order in the $d_{x^2-y^2}$ channel. For a homogeneous system this order parameter alone would be sufficient; the secondary component only becomes important once we include strain inhomogeneities. Following Ref. [16], this second component is assumed to be $g_{xy(x^2-y^2)}$. We later discuss how our results change for different subleading pairing states, such as s wave.

In an otherwise clean system, such as superconducting Sr$_2$RuO$_4$, inhomogeneous strain is most prominently induced by dislocations, i.e., a linear crystallographic defect, as shown in Fig. 1. To study the impact of dislocation-induced strain on superconductivity we consider the Ginzburg-Landau free-energy density

$$f = f_0 + f_{\text{disl}}, \tag{1}$$

where the dislocation-free contribution f_0 reads

$$f_0 = \frac{1}{2}\psi^\dagger(r_0\tau_0 - \delta T\,\tau_z)\psi + \frac{u_+}{8}(\psi^\dagger\tau_0\psi)^2 + \frac{u_-}{8}(\psi^\dagger\tau_z\psi)^2$$
$$+ \frac{v}{8}(\psi^\dagger\tau_x\psi)^2 + \frac{w}{4}(\psi^\dagger\tau_0\psi)(\psi^\dagger\tau_z\psi) + f_{\text{grad}}. \tag{2}$$

Here, $r_0 = T - T_0$ is the effective temperature, with T_0 setting a transition temperature scale. The parameters $u_\pm$, v, and w are associated with the different symmetry-allowed quartic terms. The conditions $0 < w^2 < u_+u_-$ ensure the stability of the functional. The Pauli matrices τ_i act in the space of the two-component order parameter ψ. Within a mean-field approach, the system described by Eq. (2) develops a uniform d-wave state below $T_c \equiv T_0 + \delta T$, where it picks a global $U(1)$ phase Φ. Owing to the invariance of the free energy under the transformation $\psi_d \to \psi_d$ and $\psi_g \to \psi_g^*$, the relative phase φ of the gap function

$$\Psi = e^{i\Phi}(|\psi_d| + e^{i\varphi}|\psi_g|), \tag{3}$$

becomes a $\mathbb{Z}_2$ Ising degree of freedom that can undergo its own transition. In fact, a finite expectation value of the pseudospin

$$\sigma = \text{sign}(\sin\varphi) \tag{4}$$

marks the onset of the time-reversal symmetry broken state. The condensation of the corresponding degree of freedom plays an important role in our subsequent analysis, albeit not for a homogeneous order parameter.

A uniform g-wave component ψ_g would emerge below $T_c^< \equiv T_0 - \delta T\frac{u_+ + w}{u_- + w}$, with, for $v > 0$, a phase $\varphi = \pm\pi/2$ relative to ψ_d. In the fine-tuned system where $\delta T = 0$, analyzed in Ref. [16], both order parameters develop at the same temperature. In this work we consider $\delta T \sim T_c$ sufficiently large such that the homogeneous, perfect crystal only displays one phase transition with order parameter ψ_d. Still, the expansion Eq. (2) implicitly assumes that the subleading channel ψ_g is much closer to condensation than any other pairing channel. We include the gradient terms

$$f_{\text{grad}} = \frac{\kappa_\parallel}{2}(|\partial_x\psi|^2 + |\partial_y\psi|^2) + \frac{\kappa_\perp}{2}|\partial_z\psi|^2, \tag{5}$$

where $\kappa_\parallel > \kappa_\perp$ reflects the electronic anisotropy of the material. In principle, there are additional symmetry-allowed
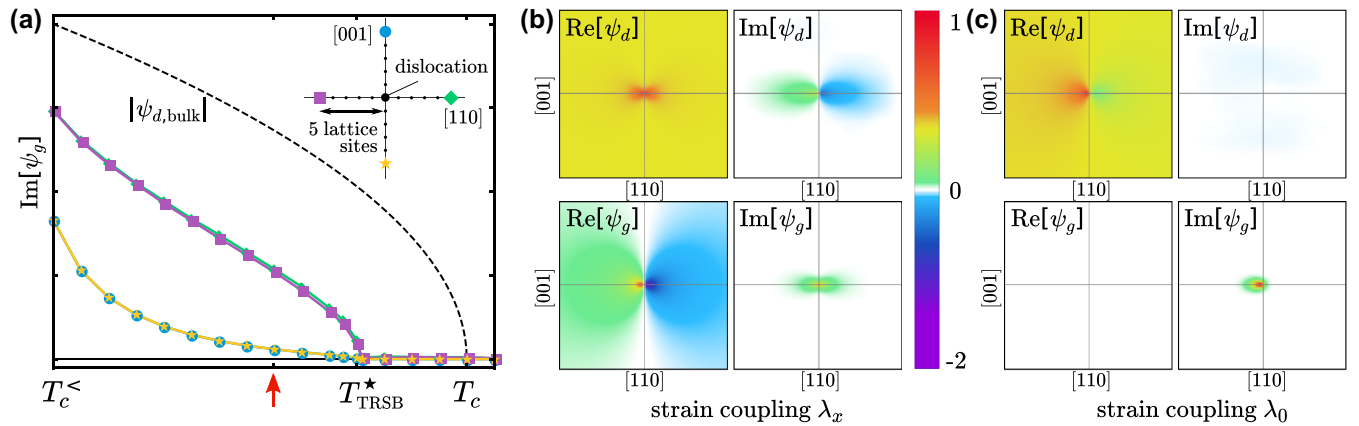
FIG. 2. Monte-Carlo simulation to minimize the Ginzburg-Landau free energy, Eq. (1), for the two order parameters in the presence of a dislocation. (a) Strain-induced onset of the imaginary part of the order parameter ψ_g at four locations (see inset) around a dislocation. Because ψ_d is already present at $T < T_c$, this onset *locally* breaks time-reversal symmetry at $T^\star_{\mathrm{TRSB}}$. Note that both these temperatures are much larger than the temperature $T_c^<$ at which the homogeneous g-wave order parameter would onset. (b),(c) Order parameter distribution near the dislocation for fixed temperature [red arrow in (a)] and for $\lambda_x = 8$ and $\lambda_0 = 5$ respectively, see Eq. (7).

gradient terms that mix the two components but that will not qualitatively alter the findings of our analysis.

We now analyze the effect of a single edge dislocation on the pairing state described by Eq. (2). Edge dislocations occur even in otherwise exceptionally clean materials and lead to strong local strain fields, yielding associated stress values of several GPa [46]. These strain fields change the local energetics of the superconductor and locally break the tetragonal lattice symmetry, mixing different pairing channels. The strain field in the vicinity of an edge dislocation is given in standard textbooks [47]. It is characterized by the Burgers vector $\boldsymbol{b} = b\hat{\boldsymbol{b}}$ and the unit vector $\hat{\boldsymbol{t}}$ tangential to the dislocation line. The strain tensor $\epsilon_{\alpha\beta} = (\partial_\alpha u_b + \partial_\beta u_\alpha)/2$ is evaluated from the displacement field $\boldsymbol{u}$. For an edge dislocation, the latter is given by

$$\boldsymbol{u} = \frac{\boldsymbol{b}}{2\pi}\left[\theta + \frac{A}{2}\sin(2\theta)\right] + \frac{\hat{\boldsymbol{t}} \times \boldsymbol{b}}{2\pi}[A\cos^2(\theta) + B\log(\rho)], \quad (6)$$

where ρ and θ are the polar coordinates in the plane perpendicular to the dislocation and the parameters A and B can be expressed in terms of elastic constants [47]. While the electronic system is very anisotropic, the elastic deformations induced by a dislocation are expected to be similar to those in an isotropic elastic system. The key implications of Eq. (6) for the strain tensor $\epsilon_{\alpha\beta}$ are that its magnitude decays like $1/\rho$, while the sign of the tensor elements depends on the orientation of $\boldsymbol{b}$ and $\hat{\boldsymbol{t}}$, similarly to the case of an electric field generated by a dipole. Quite generally then, one finds tension ($\epsilon_{\alpha\beta} > 0$) on one side of the dislocation and compression ($\epsilon_{\alpha\beta} < 0$) on the other side, following a typical dipolar angular dependence, see Ref. [47]. Based on the results of Ref. [45], we consider a Burgers vector $\boldsymbol{b} = b\hat{\boldsymbol{z}}$, see Fig. 1. Dislocations form loops or end at the sample surfaces. In what follows we consider a segment that can be considered locally as a straight dislocation line. In our specific analysis, we opt for a tangent $\hat{\boldsymbol{t}} = (\hat{\boldsymbol{x}} + \hat{\boldsymbol{y}})/\sqrt{2}$ along the crystallographic [110] direction. Except for $\hat{\boldsymbol{t}} = \hat{\boldsymbol{x}}$ (or $\hat{\boldsymbol{y}}$)—in which case ϵ_{xy} vanishes—any generic direction of $\hat{\boldsymbol{t}}$ yields a similar behavior. Transmission electron microscopy images of Sr$_2$RuO$_4$ reveal

that dislocations do not follow these high-symmetry axes and substantiate our choice [45].

The coupling between the dislocation and the superconducting order parameter can be cast in the form

$$f_{\mathrm{disl}} = \frac{1}{2}\sum_{\alpha=0,x,z}\lambda_\alpha\varepsilon^\alpha(\boldsymbol{r})\psi^\dagger(\boldsymbol{r})\tau_\alpha\psi(\boldsymbol{r}). \quad (7)$$

Hereby $\varepsilon^\alpha(\boldsymbol{r})$ denotes the projection of the spatial variation of the strain field to distinct symmetry sectors ($\alpha = 0, x, z$) and λ_α are the associated coupling constants. The A_{1g} strain components ε^0 and ε^z are linear combinations of $\epsilon_{xx} + \epsilon_{yy}$ and ϵ_{zz}. As such, they locally change the superconducting transition temperature and the degree of degeneracy between the d- and g-wave components. The experiments of Ref. [45] demonstrated that a large coupling of this kind is present in Sr$_2$RuO$_4$. In our case, the component ε^x corresponds to a B_{2g} strain, $\varepsilon^x \equiv \epsilon_{xy}$, which breaks the tetragonal lattice symmetry near the dislocation to a degree that both order parameters belong to the same irreducible representation and, hence, emerge simultaneously. The correspondence $\varepsilon^x \leftrightarrow \epsilon_{xy}$ is dictated by the product representation $B_{2g} = B_{1g} \otimes A_{2g}$ of the order parameters, see Eq. (7). Given the low symmetry of the dislocation-induced strain for a generic orientation of $\hat{\boldsymbol{t}}$ one expects that all strain components are finite. The pronounced strain dependence of the bulk superconducting transition [8,31,32] and the near doubling of the local onset of superconductivity near dislocations [45] are evidence for strong coupling constants λ_α. It is instructive to investigate the mechanism of local TRSB for pure strain couplings $\propto\lambda_\alpha$. For either λ_0 or λ_z the breaking of time-reversal symmetry is dictated by the quartic term $-v(\psi^\dagger\tau_x\psi)^2/8$ in Eq. (2). This implies that the strain-induced g-wave component develops with a phase $\pm\pi/2$ relative to the leading order. In distinction, the coupling $\propto\lambda_x$ mixes the two order parameters in a way that on opposite sides of the dislocation we find $d + g$ and $d - g$ pairing states, since the strain changes from tensile to compressive as one traverses the dislocation. Asymptotically the g-wave component decays algebraically as
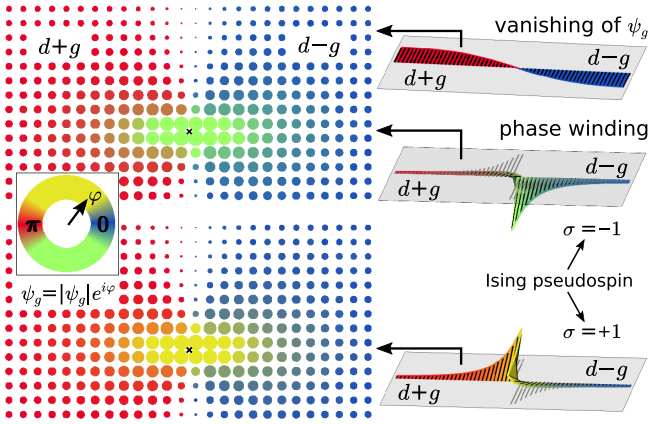
FIG. 3. Amplitude (circle size) and phase (color) of the strain-induced g-wave component in proximity to a dislocation. Here we consider λ_x to be the dominant strain-superconductivity coupling, as shown in Fig. 2(b). Inhomogeneous TRSB occurs when the phase winding (right, middle, and bottom) is energetically favored over the vanishing of the g-wave component. Away from the dislocation the magnitude of the g component is small and a direct sign change is always preferred (right, top, cut at $z = 25b$). Both degenerate solutions—distinguished by the pseudospin σ, see Eq. (4), and reflecting the Ising symmetry of the TRSB order—are shown.

$\psi_g(\boldsymbol{r}) \propto \varepsilon^x(\boldsymbol{r})\psi_d$. To connect the $d + g$ and $d - g$ regions, the g-wave component can either vanish or establish a local time-reversal symmetry broken state $d + e^{i\varphi(\boldsymbol{r})}g$ where the phase φ gradually winds from 0 to π. The system opts for the second possibility when the strain term $\pm\lambda_x \cos\varphi$ dominates over the gradient terms in Eq. (5). The mechanism is reminiscent, albeit qualitatively different, from other cases discussed in the literature where time-reversal symmetry breaking superconductivity takes place at twin boundaries of the crystal [48–50]. In distinction to Eq. (7), TRSB due to crystalline deformations through higher order gradient couplings $(\partial \varepsilon^\alpha)(\psi^\dagger \tau_\alpha \partial \psi)$ was discussed in Ref. [51].

Independent of the strain coupling, the onset of a nontrivial phase winding takes place at a well-defined temperature $T_{\mathrm{TRSB}}^\star$ and is spatially localized around the dislocation core. Indeed, the problem of determining the onset of phase winding near a dislocation can be recast as a problem of finding the condition under which a bound state emerges in a Schrödinger-type problem [52]; see Appendix B. The onset temperature of local TRSB is then larger than the temperature where a homogenous ψ_g component would appear, $T_{\mathrm{TRSB}}^\star \geqslant T_c^<$. Importantly, $f + f_{\mathrm{disl}}$ is still invariant under the transformation $\psi_d \to \psi_d$ and $\psi_g \to \psi_g^*$ and hence, the $\mathbb{Z}_2$ Ising degree of freedom remains intact. Thus, at $T_{\mathrm{TRSB}}^\star$ the system locally picks one of two degenerate solutions, solely distinguished by the Ising pseudospin $\sigma = \pm 1$, see Eq. (4). A large system with many dislocations undergoes a TRSB transition at T_{TRSB} once it locks all its Ising pseudospins σ_i in a ferromagnetically ordered state and *globally* breaks the $\mathbb{Z}_2$ symmetry. This point will be further explored in the next section, where we will show that $T_{\mathrm{TRSB}} \lesssim T_{\mathrm{TRSB}}^\star$.

We have solved the coupled nonlinear equations $\delta f/\delta \psi_d = \delta f/\delta \psi_g = 0$ for the total free energy Eq. (1) via a stochastic annealing approach. All numerical results are obtained from a Monte-Carlo simulation of a discretized system with 100×100 lattice sites (covering an area $10^3 \xi_\parallel^2$) with $u_\pm = 1 \mp 0.5$, $v = 1$, $w = 0.5$, $\kappa_\parallel \equiv \xi_\parallel^2 = 10$, $\kappa_\perp = 2$. As a result $T_c = T_0 + \delta T$ and $T_c^< = T_0 - \delta T/2$ (while T_0 remains arbitrary, we used $\delta T = 1$). A realistic description of the strain fields is achieved with the simple expression $\varepsilon^\alpha(\boldsymbol{r}) = \varepsilon^\alpha(\rho, \theta) = b\cos(\theta)/\rho$. Owing to the scale invariance of this expression, the absolute coupling strength to the lattice takes the form $\lambda_\alpha b$. To simplify the discussion we fix $b^2 = \xi_\parallel^2/10$ in the numerical procedure. The spatial distribution of the order parameters near the dislocation is shown in Fig. 2 for the limiting cases where the strain-superconductivity coupling is purely determined by λ_x [Figs. 2(a) and 2(b)] and by λ_0 [Fig. 2(c)], respectively. Figure 3 illustrates both options of connecting the $d \pm g$ regions: Near (far from) the dislocation the connection occurs via phase winding (vanishing) of ψ_g. Furthermore, it also shows the two degenerate solutions $\sigma = \pm 1$ for winding the phase between the $d + g$ and $d - g$ regions.

The dependence of $T_{\mathrm{TRSB}}^\star$ on the magnitude of the coupling constants λ_x and λ_0 is shown in Fig. 4(a). For sufficiently large strain couplings one can induce local TRSB pairing above the bulk temperature, a consequence of the fact that pairing can be boosted locally. In Fig. 4(b) we analyze the change of the bulk transition temperature T_c and of the local TRSB onset temperature $T_{\mathrm{TRSB}}^\star$ as a function of the in-plane strain $\epsilon_{B_{1g}}$, as modeled by an additional term $f_{B_{1g}} = -\epsilon_{B_{1g}}^2 \psi^\dagger (\tau_0 + \tau_z)\psi/4$. Figure 4 was obtained for the specific coupling strength $\lambda_x = 8.75$ after fine tuning $T_c \approx T_{\mathrm{TRSB}}^\star$ at zero applied strain. The superconducting transition temperature changes quadratically with strain, as is required for a single-component order parameter. $T_{\mathrm{TRSB}}^\star$ on the other hand is weakly affected by strain values that are much smaller than the local, dislocation-induced strain. Even the largest applied strain field in modern experiments amounts to stress values that are an order of magnitude smaller than typical edge-dislocation stresses [46]. This may explain why the experiments in Ref. [8] did not observe a significant change for the TRSB onset temperature with applied strain along the [100] direction.

It is also interesting to discuss what happens if strain is applied along the [110] direction (i.e., B_{2g} strain). For our scenario of inhomogeneous local TRSB at $T_{\mathrm{TRSB}}^\star$, the phase diagram of Fig. 4(b) would remain essentially unchanged. However, for the scenario of homogeneous TRSB taking place at $T_c^<$, significant changes are expected. In particular, because B_{2g} strain couples the ψ_d and ψ_g order parameters bilinearly, one would generally expect a stronger, linear enhancement of T_c and of the separation between T_c and the TRSB transition temperature with increasing B_{2g} strain.

To discuss what happens in the presence of an external magnetic field H_z along the z direction, we note that it transforms according to the A_{2g} irreducible representation and that it is odd under time reversal. Consequently, there is an additional term in f_{disl}

$$f_{\mathrm{disl}} \to f_{\mathrm{disl}} - H_z \lambda_y \varepsilon^y(\boldsymbol{r})\psi^\dagger(\boldsymbol{r})\tau_y \psi(\boldsymbol{r})/2, \qquad (8)$$

where $\varepsilon^y = \epsilon_{x^2-y^2}$ is the projection of the strain field onto the B_{1g} channel. This coupling is crucial to explain the finite Kerr signal observed in Ref. [9], as it allows one to train different regions of broken time-reversal symmetry with a magnetic field. The condition of a broken vertical mirror symmetry
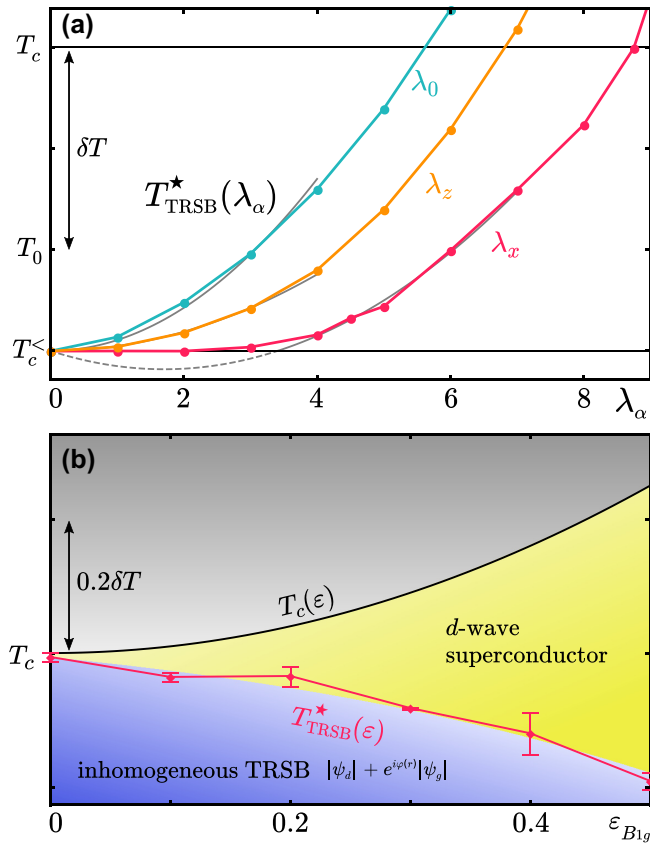
FIG. 4. (a) Evolution of $T_{\mathrm{TRSB}}^{\star}$ upon varying the interaction parameters λ_0, λ_z, and λ_x. Recall that T_c ($T_c^<$) is the temperature at which a homogeneous ψ_d (ψ_g) component sets in, and $T < T_c^<$ results in a uniform time-reversal symmetry broken state. The analytic results (gray curve) indicate that $T_{\mathrm{TRSB}}^{\star}(\lambda_{0,z})$ deviates quadratically away from $T_c^<$. Meanwhile, $T_{\mathrm{TRSB}}^{\star}(\lambda_x)$ deviates from $T_c^<$ only above a threshold value. (b) Phase diagram as function of homogeneous B_{1g} strain and temperature. It is evaluated for $\lambda_x = 8.75$ and for $T_c(0) = T_{\mathrm{TRSB}}^{\star}(0)$. The analytic relation $T_c(\epsilon) - T_c(0) = (\delta T^2 + \epsilon^2)^{1/2}$ is shown in black.

to achieve a finite Kerr signal is naturally fulfilled near the dislocation.

Let us finally discuss what would happen for different combinations of single-component order parameters. Consider the case $\psi = (\psi_d, \psi_s)$ with a second component transforming as A_{1g}, i.e., s wave. Then, the symmetry-mixing strain in Eq. (7) is given by $\varepsilon^x = \epsilon_{x^2-y^2}$ since $B_{1g} = B_{1g} \otimes A_{1g}$. Other than that, our analysis would be largely unchanged. On the other hand if one considered the case of $d_{x^2-y^2}$ and d_{xy} states, no strain mixing term ε^x is allowed, because $A_{2g} = B_{1g} \otimes B_{2g}$ and there is no A_{2g} strain in the D_{4h} point group. The same is true for a combination of s-wave with g-wave pairing. Hence, the presented scenario applies to combinations of d with either g- or s-wave states. The time-reversal symmetry-broken state of all combinations of single-component order parameters can be trained with a magnetic field H_z, since the strain fields induced by the dislocation always contain a component that couples H_z with the two components of ψ.

Thus far, we established the occurrence of phase winding near a single dislocation and determined the onset
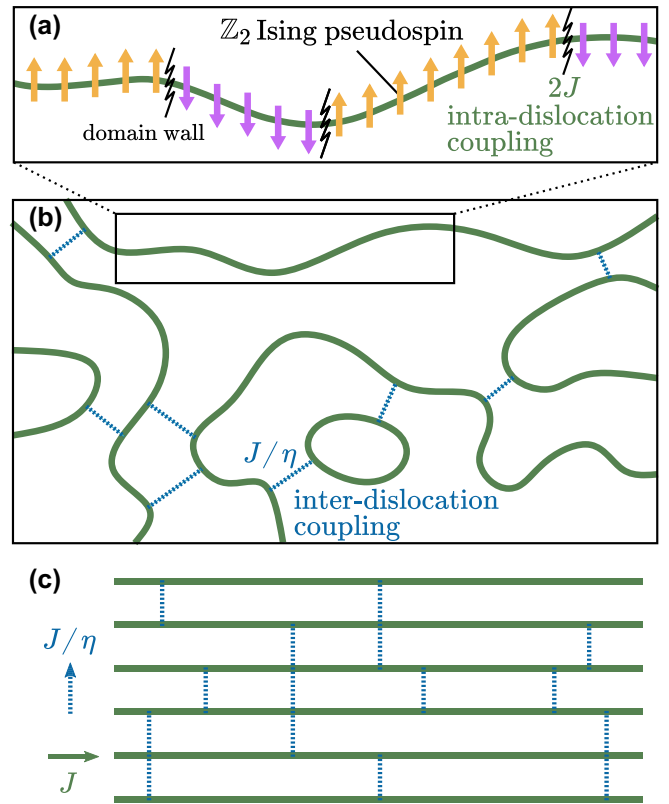

FIG. 5. Mapping of the physical system to an effective coarse-grained model. Panel (a) shows the Ising domain walls associated with the Ising TRSB order parameter of Eq. (4), which proliferate along a dislocation line according to the 1D Ising model. Panel (b) illustrates the coupling between multiple dislocations, which can form open lines connecting the surfaces of the sample of closed loops. As a result, as shown in panel (c), the critical behavior of the model is the same as that of an anisotropic 2D Ising model with exchange parameters J and J/η, with $\eta \gg 1$.

temperature scale $T_{\mathrm{TRSB}}^{\star}$ for this behavior. The local breaking of time-reversal symmetry—marked by a nonvanishing $|\psi_g| \sin(\varphi)$—takes place in a finite region around the core of the dislocation. In the next section we allow for the Ising variable σ to vary in space along the dislocation line and between different edge dislocations.

C. Collective excitations and global phase transition for many dislocations

In this section we analyze the case of many coupled dislocations. We find that this leads to a sharp TRSB phase transition in the Ising universality class at a temperature T_{TRSB}. Given the underlying Ising symmetry, it is however possible that the phase variable undergoes a thermally excited kink $\varphi \to 2\pi n - \varphi$ along the dislocation line. In terms of the Ising variable σ, see Eq. (4), the kink corresponds to a domain wall, as illustrated in Fig. 5(a). In a coarse-grained approach, the statistical mechanics of a single dislocation maps to a one-dimensional Ising chain
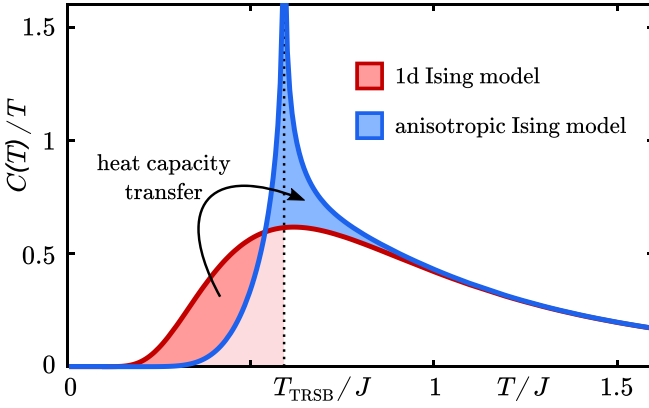
$$H_1 = -J \sum_i^N \sigma_i \sigma_{i+1}, \tag{9}$$

FIG. 6. Entropy change $C(T)/T$ per Ising pseudospin (in units of k_B/J) of the anisotropic Ising model with $J'/J = 0$ (red) and 0.01 (blue). This illustrates our approach to estimate the total weight of the heat-capacity anomaly at the transition for finite J' from the transferred calorimetric weight in $C_{\text{Ising},d=1}/T$.

where the dislocation is divided along its length L in $N = L/\ell$ segments of typical length ℓ. Each segment is associated with a local Ising spin σ_i and a binding energy per unit length J. The characteristic values

$$\ell \sim (\kappa_\parallel \kappa_\perp)^{1/2}/\lambda_\alpha b \qquad (10)$$

and $J \sim T^*_{\text{TRSB}}$ follow from the aforementioned solutions of the Schrödinger equations, see Appendix B. For the one-dimensional Ising model it holds that $\langle \sigma \rangle = 0$ at any finite temperature. The density of kinks per unit length, $n_{\text{kink}} \sim -\ell^{-1} \log[\tanh(2J/T)]$, is exponentially small at low T. Shorter dislocation loops, with $N < e^{2J/T}$, have negligible probability for kinks and are essentially ordered. However, averaging over many uncoupled loops gives rise to a vanishing global order parameter $\langle \sigma \rangle$.

To account for the coupling between distinct dislocations, we note that the magnitude of local TRSB decays exponentially as $e^{-\rho/\ell}$ in the direction transverse to the dislocation. Then, two dislocation segments at a distance ρ will interact via the exponentially small coupling $J'(\rho) = Je^{-\rho/\ell}$. From an analysis of the gradient terms of the Ginzburg-Landau expansion, it follows that the sign of this interaction is ferromagnetic. The many-dislocation problem is therefore governed by the coarse-grained Hamiltonian

$$H = \sum_m H_1^m + \sum_{m,m'} \sum_{i,j} J'(\rho_{i,j})\sigma_i^m \sigma_j^{m'}. \qquad (11)$$

The superscripts m, m' label the dislocation, and $\rho_{i,j}$ denotes the distance between the segments i (of dislocation m) and j (of dislocation m').

Owing to the exponential dependence of the coupling $J'(\rho)$, one can further map the problem to an anisotropic Ising model with coupling constant J in one direction and a single coupling constant J/η in the orthogonal directions. Here $\eta = e^{\bar\rho/\ell}$ with $\bar\rho$ the typical value for the shortest distance of two neighboring dislocations. This is shown in panels (b) and (c) of Fig. 5. The anisotropic Ising model develops a finite order parameter $\langle \sigma \rangle$ below the transition temperature

$$T_{\text{TRSB}} \sim J/\ln(\eta) \sim (\ell/\bar\rho)T^\star_{\text{TRSB}}. \qquad (12)$$

This result follows regardless of whether the coupling via J' leads to a two- or three-dimensional network of dislocations. It is a consequence of the one-dimensional Ising model being at its lower critical dimension. The above expression implicitly assumes a weak coupling between nearby dislocations, i.e., $\ell < \bar\rho$. In that case the transition temperature T_{TRSB} is smaller than, but potentially comparable to, the local ordering temperature $T^\star_{\text{TRSB}}$. While the ordering of single dislocations is hindered by kinks along the loop, the weak dislocation-dislocation coupling locks the global Ising variable and leads to a global symmetry breaking.

The heat-capacity anomaly associated with the lifting of the $\mathbb{Z}_2$ symmetry is much smaller in magnitude than the one due to the opening of the single particle gap at the bulk superconducting transition temperature T_c. To show this, we estimate the change of the electronic specific heat at the superconducting transition as $\Delta C(T_c) \sim S_{\text{el}}(T_c) \sim T_c/\epsilon_F$, with S_{el} the electronic contribution to the entropy and ϵ_F the Fermi energy (the Boltzmann constant k_B is set to unity). In contrast, the heat capacity per Ising spin of an anisotropic two-dimensional Ising model follows from Onsager's solution and is shown in Fig. 6. The extent of the calorimetric anomaly at T_{TRSB} (blue shaded area in Fig. 6) corresponds to the heat-capacity transfer (dark red area in Fig. 6). To estimate the magnitude of this effect, we use the approximate form

$$\delta S_{\text{TRSB}} \approx \int_0^{T_{\text{TRSB}}} \frac{C_{\text{Ising},d=1}(T')}{T'} dT', \qquad (13)$$

with the heat capacity of the one-dimensional Ising model

$$C_{\text{Ising},d=1} = \frac{a^2 c}{\bar\rho^2 \ell} \frac{J^2}{T^2[\cosh(J/T)]^2}. \qquad (14)$$

The expression in Eq. (13) accounts for the total red area in Fig. 6. Here a and c are the in-plane and out-of-plane lattice constants. The small prefactor $a^2 c/(\bar\rho^2 \ell)$ accounts for the number of Ising pseudospins per unit cell and is needed to compare with the electronic contribution. Using Eq. (10) and the dimensionless coupling $\bar\lambda_\alpha = \lambda_\alpha/T_c$ we find $\ell = (a/\bar\lambda_\alpha)(\epsilon_F/T_c)^2$ and obtain the ratio

$$\frac{\delta S_{\text{TRSB}}}{S_{\text{el}}(T_c)} \sim \frac{1}{S_{\text{el}}(T_c)} \frac{a^2 c}{\bar\rho^2 \ell} \frac{\log \eta}{\eta^2} \sim \bar\lambda_\alpha^2 \frac{a}{\bar\rho} \left(\frac{T_c}{\epsilon_F}\right)^3 e^{-2\bar\rho/\ell}. \qquad (15)$$

As anticipated, the entropy associated with the collective phase locking, and thus to the TRSB transition, is—in addition to the two small prefactors $(T_c/\epsilon_F)^3$ and $(a/\bar\rho)$—exponentially suppressed.

Our conclusion of a global Ising transition at T_{TRSB} can also be reached by considering disorder that is caused by dislocations at random positions and with random Burgers-vector orientations [53]. From Eq. (7) it follows that dislocation strain acts like a uniaxial random field that couples to $\cos[\varphi(r)]$, with the relative phase $\varphi(r)$, see Eq. (3). The corresponding XY model with random uniaxial field is a well-studied problem in the statistical mechanics of disordered systems, with several rigorous results [54–60]. It undergoes an Ising transition with order parameter $\langle \cos[\varphi(r)] \rangle \neq 0$, fully consistent with our analysis. This demonstrates that our conclusions concerning the nature of the transition as clean Ising

transition are robust despite the random nature of the dislocation problem.

III. DISCUSSION

In this paper we proposed an alternative origin for the observed breaking of time-reversal symmetry in Sr_2RuO_4 due to inhomogeneous strain fields that locally couple a single-component primary order parameter to a subleading pairing state. While the material without strain inhomogeneities would only display the primary order, which is likely of $d_{x^2-y^2}$ symmetry, strong strain fields mix these symmetry-distinct pairing states. A promising candidate for such strain inhomogeneities are those originated near edge dislocations as shown in Fig. 1. Local stress values near such dislocations are easily in the regime of several GPa, leading to a strong order-parameter mixing. Compressive and tensile strain on opposite sides of the dislocation are then shown to lead to local TRSB via phase winding of the induced pairing wave function. The main appeal and ultimate motivation for this proposal is the absence of a mean-field behavior of the heat capacity at T_{TRSB} under homogeneous strain, while such behavior occurs at T_c. A scenario which attributes TRSB to the opening of an additional pairing gap would directly affect the entropy of electronic quasiparticles. The fact that no heat-capacity jump is experimentally detected at T_{TRSB} is a strong evidence against any such scenario.

There are certain similarities, but also important differences between our theory and the description of Ref. [16] advocating an accidental degeneracy of homogeneous d- and g-wave pairing. In both cases two symmetry distinct states are relevant and time-reversal symmetry breaking is a consequence of the relative phase between these two states. In both descriptions one has to fine tune $T_{TRSB} \approx T_c$ for unstrained samples. There are, however, significant distinctions. First, in our approach it is in principle possible to observe time-reversal symmetry broken states via local probes even above T_c. This effect is a consequence of the local enhancement of pairing near dislocations, as reported by experiments [45]. Second, our findings suggest that TRSB may be engineered by controlling the dislocation density during sample preparation, which in principle allows for a clearer separation between T_c and T_{TRSB}. Evidence for a sample dependence of T_{TRSB}, and even of $T_{TRSB} > T_c$, was reported in Ref. [8]. Third, we do not expect a strong heat-capacity anomaly at T_{TRSB}. In our description, time-reversal symmetry breaking is a phase locking process where comparatively few degrees of freedom are involved and no gap opening of single particle states occurs. As a result, the transition leaves weak signatures in the heat-capacity signal and hence, naturally explains the absent heat-capacity anomaly at T_{TRSB} found in strained samples [21]. In the case of a homogeneous $d+ig$ state [16] one would expect a jump in the heat capacity at the second bulk transition. Finally, a prediction that may be used to falsify our theory in future experiments is the change of the transition temperature T_c with uniaxial strain $\epsilon_{B_{1g}}$ and $\epsilon_{B_{2g}}$. We expect that T_c changes quadratically with strain for both symmetries, while Ref. [16] clearly predicts a quadratic variation with $\epsilon_{B_{1g}}$ but a linear change with $\epsilon_{B_{2g}}$. An investigation of $T_c(\epsilon_{B_{2g}})$ should be able to discriminate between the two scenarios. A_{1g} strain renormalizes all terms in the Ginzburg-Landau expansion. No symmetry arguments can therefore explain the apparent coincidence of T_{TRSB} and T_c under hydrostatic pressure [61].

An important observation that concerns the pairing state of Sr_2RuO_4 is the discontinuity of the elastic constant C_{66} at the superconducting transition temperature [13,14], see also Ref. [38]. Elastic constants associated with strain that transforms trivially, i.e., according to A_{1g}, are expected to be discontinuous at any superconducting transition [62]. However, elastic constants like C_{66} or $C_{11} - C_{12}$, corresponding to B_{1g} or B_{2g} strain, respectively, are continuous for a single-component order parameter. A jump of these elastic constants then clearly signals a multicomponent order parameter [63]. Nevertheless, they should not be taken as irrevocable evidence for a homogeneous two-component order parameter. Given the slowly decaying dislocation-induced g-wave component, the system is according to our theory essentially a two-component order parameter for large parts of the sample. Our analysis of single dislocations shows clearly that the regions of the sample with local $d \pm g$ pairing, that should affect the elastic constant jump, are much larger than the regions near the core of the dislocation, where time reversal symmetry is broken. This gives rise to a discontinuity of C_{66} while $C_{11} - C_{12}$ should be continuous or at best have a much smaller jump consistent with Refs. [13,14,38]. Quantitatively, the scattering of elastic waves off dislocations is strong [64,65] and gives rise to corrections of the elastic constants of the order of 10^{-2} [66]. These effects are much larger than the largest observed relative magnitudes of the discontinuities of Ref. [13], which are of the order of 10^{-4}. Finally, the size of the reported jump of C_{66} in different measurements (compare Refs. [13] and [14]) varies significantly, by about two orders of magnitude. While this may partially be due to the different experimental techniques used, sample-to-sample variations of the effect follow very naturally within our theory.

Our proposed scenario for the origin of TRSB in Sr_2RuO_4 could also be tested by experiments in plastically deformed samples. In contrast to elastic strain, plastic strain is known to create, move, and combine dislocations. It was recently observed that the transition temperature of another superconducting perovskite, $SrTiO_3$, increased substantially upon application of plastic strain, a behavior attributed to the formation of self-organized dislocation structures [67]. In Sr_2RuO_4, an enhancement of the dislocation density by plastic strain would likely result in a larger TRSB signal. Even if the dominant effect of plastic deformation is to combine and merge the existing dislocations, one would still expect a significant change of the TRSB signal. Manipulating this unconventional superconductor via plastic deformation may therefore be utilized to strain engineer the degree of time-reversal symmetry breaking in the sample.

ACKNOWLEDGMENTS

APPENDIX A: HEAT CAPACITY OF TWO DEGENERATE SUPERCONDUCTORS

The primary motivation for our analysis was the absence of a signature in the heat capacity at the time-reversal symmetry breaking transition of strained samples [21], where μSR experiments find that T_c and T_{TRSB} are distinct transitions [8]. In this Appendix we briefly summarize the heat-capacity anomalies for homogeneous two-component order parameters. We use the Ginzburg-Landau expansion of Eq. (2). For $\delta T = 0$ one should distinguish between an order parameter that belongs to a two-dimensional irreducible representation, such as E_g or E_u, and two accidentally degenerate order parameters that each belong to one-dimensional irreducible representations. From the perspective of the heat capacity, the former is a special case of the latter where the quartic coupling constant w in Eq. (2) vanishes.

For degenerate order parameters holds $\delta T = 0$, and $T_c = T_0$. The discontinuity of the heat capacity is

$$\frac{\Delta C(T_0)}{T_0} = \frac{u_-}{u_+ u_- - w^2}. \tag{A1}$$

Let us now analyze finite δT, i.e., the degeneracy is lifted. The upper transition temperature is $T_c = T_0 + \delta T$ with heat-capacity jump

$$\frac{\Delta C_1(T_c)}{T_c} = \frac{1}{u_+ + u_- + 2w}. \tag{A2}$$

The lower transition temperature is $T_c^< = T_0 - \frac{u_+ + w}{u_- + w}\delta T$ and the corresponding heat capacity jump is

$$\frac{\Delta C_2(T_c^<)}{T_c^<} = \frac{(u_- + w)^2}{u_- u_+ - w^2}\frac{\Delta C_1(T_c)}{T_c}. \tag{A3}$$

Let us first focus on the case when δT lifts the degeneracy of a two-dimensional irreducible representation. In this situation it holds $w = 0$. It then follows that the ratio of the heat capacities at the two transitions equals the ratio of the slopes

of the transition temperatures

$$\frac{\Delta C_2(T_c^<)}{\Delta C_1(T_c)} = \frac{u_-}{u_+} = \frac{\frac{dT_c}{\delta T}}{\left|\frac{dT_c^<}{\delta T}\right|}. \tag{A4}$$

If both temperatures split evenly, the heat-capacity jumps at the two transitions have to be the same. If the upper transition departs more rapidly away from T_0—which seems to be the case for Sr_2RuO_4—then the lower heat-capacity jump should be the larger one. This is in sharp disagreement with experiments of Ref. [21]. More freedom is left if two symmetry-distinct order parameters are degenerate by accident and $w \neq 0$ is allowed. Now a negligible second calorimetric jump is possible if $w = -u_-$. However, this condition implies that the second component, i.e., the g-wave order parameter, develops negligible amplitude, i.e., superconductivity prefers to order with ψ_d finite but $\psi_g \approx 0$.

APPENDIX B: SCHRÖDINGER BOUND-STATE PROBLEM

To illustrate the mapping of the local TRSB to the appearance of a bound state in a Schrödinger-type problem we focus on the case with pure λ_0 coupling. We further assume that the system has developed a bulk d-wave component ψ_d (we assume ψ_d to be real). Note, this assumption is made to simplify the following analytic reasoning and thereby limits its applicability to the case $T_{\text{TRSB}}^\star \leqslant T_c$. In general however, local TRSB can occur even above the bulk superconducting transition, i.e., $T_{\text{TRSB}}^\star > T_c$, see Fig. 4(a). The Ginzburg-Landau equation for the imaginary part $\psi_{g,i} \equiv \text{Im}[\psi_g]$ now reads

$$\kappa \nabla^2 \psi_{g,i} = (r_0 + \delta T + \lambda_0 \varepsilon^0)\psi_{g,i} + [(u_+ + u_-)/2]\psi_{g,i}^3. \tag{B1}$$

For simplicity we chose $\kappa \equiv \kappa_\parallel = \kappa_\perp$. The parameter κ relates to the superconducting coherence length $\xi \sim (\epsilon_F/T_c)a$ via $\kappa \sim \xi^2 T_c$. The cubic term in $\psi_{g,i}$ may be neglected when identifying the transition temperature; this term is relevant to normalizing the bound-state wave function. The problem can then be cast in the form of a Schrödinger equation

$$\mathcal{H}\Psi = E\Psi \tag{B2}$$

with $\mathcal{H} = -\nabla^2 + V(\mathbf{r})$, $V(\mathbf{r}) = \lambda_0 \varepsilon^0/\kappa$, and $E = -(r_0 + \delta T)/\kappa$. As strain decays with a power law b/r away from the dislocation, the potential is of Coulomb type, i.e., $V(\mathbf{r}) = (\ell/r)\cos(\theta)$, with a characteristic length scale $\ell^2 = \kappa/b\lambda_0$. For $\kappa_\parallel \neq \kappa_\perp$, κ should be replaced by the geometric average $(\kappa_\parallel \kappa_\perp)^{1/2}$ as done in the expression for ℓ given in Eq. (10). The above Schrödinger problem has a well-defined ground-state energy E_0, where a bound state is realized. As temperature is lowered, the effective energy E increases until reaching E_0. This defines $T = T_{\text{TRSB}}^\star$.

[1] D. A. Wollman, D. J. Van Harlingen, W. C. Lee, D. M. Ginsberg, and A. J. Leggett, Experimental Determination of the Superconducting Pairing State in YBCO from the Phase Coherence of YBCO-Pb dc SQUIDs, Phys. Rev. Lett. **71**, 2134 (1993).

[2] C. C. Tsuei, J. R. Kirtley, C. C. Chi, Lock See Yu-Jahnes, A. Gupta, T. Shaw, J. Z. Sun, and M. B. Ketchen, Pairing Symmetry and Flux Quantization in a Tricrystal Superconducting Ring of YBa$_2$Cu$_3$O$_{7-\delta}$, Phys. Rev. Lett. **73**, 593 (1994).

[3] Y. Maeno, H. Hashimoto, and K. Yoshida, S. Nishizaki, T. Fujita, J. G. Bednorz, and F. Lichtenberg, Superconductivity in a layered perovskite without copper, Nature (London) **372**, 532 (1994).

[4] J. Mravlje, M. Aichhorn, T. Miyake, K. Haule, G. Kotliar, and A. Georges, Coherence-Incoherence Crossover and the Mass-Renormalization Puzzles in Sr_2RuO_4, Phys. Rev. Lett. **106**, 096401 (2011).

[5] T. M. Rice and M. Sigrist, Sr_2RuO_4: an electronic analogue of 3He?, J. Phys.: Condens. Matter **7**, L643 (1995).

[6] G. Baskaran, Why is Sr_2RuO_4 not a high T_c superconductor? Electron correlation, Hund's coupling and p-wave instability, Physica B **223**, 490 (1996).

[7] G. M. Luke, Y. Fudamoto, K. M. Kojima, M. I. Larkin, J. Merrin, B. Nachumi, Y. J. Uemura, Y. Maeno, Z. Q. Mao, Y. Mori, H. Nakamura, and M. Sigrist, Time-reversal symmetry-breaking superconductivity in Sr_2RuO_4, Nature (London) **394**, 558 (1998).

[8] V. Grinenko, S. Ghosh, R. Sarkar, J.-C. Orain, A. Nikitin, M. Elender, D. Das, Z. Guguchia, F. Brückner, M. E. Barber, J. Park, N. Kikugawa, D. A. Sokolov, J. S. Bobowski, T. Miyoshi, Y. Maeno, A. P. Mackenzie, H. Luetkens, C. W. Hicks, and H.-H. Klauss, Split superconducting and time-reversal symmetry-breaking transitions, and magnetic order in Sr_2RuO_4 under uniaxial stress, Nat. Phys. **17**, 748 (2021).

[9] J. Xia, Y. Maeno, P. T. Beyersdorf, M. M. Fejer, and A. Kapitulnik, High Resolution Polar Kerr Effect Measurements of Sr_2RuO_4: Evidence for Broken Time-Reversal Symmetry in the Superconducting State, Phys. Rev. Lett. **97**, 167002 (2006).

[10] A. Pustogow, Y. Luo, A. Chronister, Y.-S. Su, D. A. Sokolov, F. Jerzembeck, A. P. Mackenzie, C. W. Hicks, N. Kikugawa, S. Raghu, E. D. Bauer, and S. E. Brown, Constraints on the superconducting order parameter in Sr_2RuO_4 from oxygen-17 nuclear magnetic resonance, Nature (London) **574**, 72 (2019).

[11] K. Ishida, M. Manago, K. Kinjo, and Y. Maeno, Reduction of the ^{17}O knight shift in the superconducting state and the heat-up effect by NMR pulses on Sr_2RuO_4, J. Phys. Soc. Jpn. **89**, 034712 (2020).

[12] A. Chronister, A. Pustogow, N. Kikugawa, D. A. Sokolov, F. Jerzembeck, C. W. Hicks, A. P. Mackenzie, E. D. Bauer, and S. E. Brown, Evidence for even parity unconventional superconductivity in Sr_2RuO_4, Proc. Nat. Acad. Sci. (USA) **118**, e2025313118 (2021).

[13] S. Ghosh, A. Shekhter, F. Jerzembeck, N. Kikugawa, D. A. Sokolov, M. Brando, A. P. Mackenzie, C. W. Hicks, and B. J. Ramshaw, Thermodynamic evidence for a two-component superconducting order parameter in Sr_2RuO_4, Nat. Phys. **17**, 199 (2021).

[14] S. Benhabib, C. Lupien, I. Paul, L. Berges, M. Dion, M. Nardone, A. Zitouni, Z. Q. Mao, Y. Maeno, A. Georges, L. Taillefer, and C. Proust, Ultrasound evidence for a two-component superconducting order parameter in Sr_2RuO_4, Nat. Phys. **17**, 194 (2021).

[15] H. G. Suh, H. Menke, P. M. R. Brydon, C. Timm, A. Ramires, and D. F. Agterberg, Stabilizing even-parity chiral superconductivity in Sr_2RuO_4, Phys. Rev. Research **2**, 032023(R) (2020).

[16] S. A. Kivelson, A. C. Yuan, B. J. Ramshaw, and R. Thomale, A proposal for reconciling diverse experiments on the superconducting state in Sr_2RuO_4, npj Quantum Mater. **5**, 43 (2020).

[17] A. T. Rømer, D. D. Scherer, I. M. Eremin, P. J. Hirschfeld, and B. M. Andersen, Knight Shift and Leading Superconducting Instability from Spin Fluctuations in Sr_2RuO_4, Phys. Rev. Lett. **123**, 247001 (2019).

[18] R. Willa, Symmetry-mixed bound-state order, Phys. Rev. B **102**, 180503(R) (2020).

[19] T. Scaffidi, Degeneracy between even- and odd-parity superconductivity in the quasi-1D Hubbard model and implications for Sr_2RuO_4, arXiv:2007.13769.

[20] I. Zutic and I. Mazin, Phase-Sensitive Tests of the Pairing State Symmetry in Sr_2RuO_4, Phys. Rev. Lett. **95**, 217004 (2005).

[21] Y.-S. Li, N. Kikugawa, D. A. Sokolov, F. Jerzembeck, A. S. Gibbs, Y. Maeno, C. W. Hicks, M. Nicklas, and A. P. Mackenzie, High sensitivity heat capacity measurements on Sr_2RuO_4 under uniaxial pressure, arXiv:1906.07597.

[22] R. Sharma, S. D. Edkins, Z. Wang, A. Kostin, C. Sow, Y. Maeno, A. P. Mackenzie, J. C. S. Davis, and V. Madhavan, Momentum-resolved superconducting energy gaps of Sr_2RuO_4 from quasiparticle interference imaging, Proc. Natl. Acad. Sci. **117**, 5222 (2020).

[23] L.-D. Zhang, W. Huang, F. Yang, and H. Yao, Superconducting pairing in Sr_2RuO_4 from weak to intermediate coupling, Phys. Rev. B **97**, 060510(R) (2018).

[24] A. Bardasis and J. R. Schrieffer, Excitons and plasmons in superconductors, Phys. Rev. **121**, 1050 (1961).

[25] M. Sigrist and K. Ueda, Phenomenological theory of unconventional superconductivity, Rev. Mod. Phys. **63**, 239 (1991).

[26] T. Nomura and K. Yamada, Perturbation theory of spin-triplet superconductivity for Sr_2RuO_4, J. Phys. Soc. Jpn. **69**, 3678 (2000).

[27] Q. H. Wang, C. Platt, Y. Yang, C. Honerkamp, F. C. Zhang, W. Hanke, T. M. Rice, and R. Thomale, Theory of superconductivity in a three-orbital model of Sr_2RuO_4, Europhys. Lett. **104**, 17013 (2013).

[28] S. Raghu, A. Kapitulnik, and S. A. Kivelson, Hidden Quasi-One-Dimensional Superconductivity in Sr_2RuO_4, Phys. Rev. Lett. **105**, 136401 (2010).

[29] T. Scaffidi, J. C. Romers, and S. H. Simon, Pairing symmetry and dominant band in Sr_2RuO_4, Phys. Rev. B **89**, 220510(R) (2014).

[30] W. Huang, Y. Zhou, and H. Yao, Exotic Cooper pairing in multiorbital models of Sr_2RuO_4, Phys. Rev. B **100**, 134506 (2019).

[31] C. W. Hicks, D. O. Brodsky, E. A. Yelland, A. S. Gibbs, J. A. N. Bruin, M. E. Barber, S. D. Edkins, K. Nishimura, S. Yonezawa, Y. Maeno, and A. P. Mackenzie, Strong increase of T_c of Sr_2RuO_4 under both tensile and compressive strain, Science **344**, 283 (2014).

[32] C. A. Watson, A. S. Gibbs, A. P. Mackenzie, C. W. Hicks, and K. A. Moler, Micron-scale measurements of low anisotropic strain response of local T_c in Sr_2RuO_4, Phys. Rev. B **98**, 094521 (2018).

[33] V. P. Mineev, Broken time-reversal symmetry in the superconducting state of Sr_2RuO_4, Phys. Rev. B **76**, 212501 (2007).

[34] C. Kallin, Chiral p-wave order in Sr_2RuO_4, Rep. Prog. Phys. **75**, 042501 (2012).

[35] A. P. Mackenzie, T. Scaffidi, C. W. Hicks, and Y. Maeno, Even odder after twenty-three years: the superconducting order parameter puzzle of Sr_2RuO_4, npj Quantum Mater. **2**, 40 (2017).

[36] I. Schnell, I. I. Mazin, and A. Y. Liu, Unconventional superconducting pairing symmetry induced by phonons, Phys. Rev. B **74**, 184503 (2006).

[37] W. Cho, R. Thomale, S. Raghu, and S. A. Kivelson, Band structure effects on the superconductivity in Hubbard models, Phys. Rev. B **88**, 064505 (2013).

[38] N. Okuda, T. Suzuki, Z. Mao, Y. Maeno, and T. Fujita, Unconventional strain dependence of superconductivity in spin-triplet superconductor Sr_2RuO_4, J. Phys. Soc. Jpn. **71**, 1134 (2002).

[39] E. Hassinger, P. Bourgeois-Hope, H. Taniguchi, S. R. de Cotret, G. Grissonnanche, M. S. Anwar, Y. Maeno, N. Doiron-Leyraud, and L. Taillefer, Vertical Line Nodes in the Superconducting Gap Structure of Sr_2RuO_4, Phys. Rev. X **7**, 011032 (2017).

[40] A. P. Mackenzie and Y. Maeno, The superconductivity of Sr_2RuO_4 and the physics of spin-triplet pairing, Rev. Mod. Phys. **75**, 657 (2003).

[41] A. P. Mackenzie, R. K. W. Haselwimmer, A. W. Tyler, G. G. Lonzarich, Y. Mori, S. Nishizaki, and Y. Maeno, Extremely Strong Dependence of Superconductivity on Disorder in Sr_2RuO_4, Phys. Rev. Lett. **80**, 161 (1998); **80**, 3890(E) (1998).

[42] O. Gingras, R. Nourafkan, A.-M. S. Tremblay, and M. Côté, Superconducting Symmetries of Sr_2RuO_4 from First-Principles Electronic Structure, Phys. Rev. Lett. **123**, 217005 (2019).

[43] H. S. Røising, T. Scaffidi, F. Flicker, G. F. Lange, and S. H. Simon, Superconducting order of Sr_2RuO_4 from a three-dimensional microscopic model, Phys. Rev. Research **1**, 033108 (2019).

[44] A. A. Husain, M. Mitrano, M. S. Rak, S. I. Rubeck, H. Yang, C. Sow, Y. Maeno, P. E. Batson, and P. Abbamonte, Coexisting fermi liquid and strange metal phenomena in Sr_2RuO_4, arXiv:2007.06670.

[45] Y. A. Ying, N. E. Staley, Y. Xin, K. Sun, X. Cai, D. Fobes, T. J. Liu, Z. Q. Mao, and Y. Liu, Enhanced spin-triplet superconductivity near dislocations in Sr_2RuO_4, Nat. Commun. **4**, 2596 (2013).

[46] D. Hull and D. J. Bacon, *Introduction to Dislocations*, 3rd ed. (Pergamon, Oxford, 1984).

[47] L. D. Landau and E. M. Lifshitz, *Theory of Elasticity* (Pergamon, New York, 1986).

[48] D. L. Feder, A. Beardsall, A. J. Berlinsky, and C. Kallin, Twin boundaries in *d*-wave superconductors, Phys. Rev. B **56**, R5751 (1997).

[49] W. Belzig, C. Bruder, and M. Sigrist, Quasiclassical Theory of Twin Boundaries in High-T_c Superconductors, Phys. Rev. Lett. **80**, 4285 (1998).

[50] M. Sigrist and D. F. Agterberg, The role of domain walls on the vortex creep dynamics in unconventional superconductors, Prog. Theor. Phys. **102**, 965 (1999).

[51] A. B. Kuklov, Deformation-induced time-reversal symmetry breaking in *d*-wave superconductors, Phys. Rev. B **52**, R7002 (1995).

[52] A. R. Massih, Second-phase nucleation on an edge dislocation, Philos. Mag. **91:31**, 3961 (2011).

[53] S. A. Kivelson, private communication.

[54] A. Aharony, Spin-flop multicritical points in systems with random fields and in spin glasses, Phys. Rev. B **18**, 3328 (1978).

[55] B. J. Minchau and R. A. Pelcovits, Two-dimensional XY model in a random uniaxial field, Phys. Rev. B **32**, 3081 (1985).

[56] D. E. Feldman, Exact zero-temperature critical behaviour of the ferromagnet in the uniaxial random field, J. Phys. A: Math. Gen. **31**, L177 (1998).

[57] D. E. Feldman, Critical behavior of a degenerate ferromagnet in a uniaxial random field: Exact results in a space of arbitrary dimension, J. Exp. Theor. Phys. **88**, 1170 (1999).

[58] N. Crawford, Random field induced order in low dimension, Europhys. Lett. **102**, 36003 (2013).

[59] N. Crawford, Random field induced order in low dimension I, Commun. Math. Phys. **328**, 203 (2014).

[60] A. Bera, D. Rakshit, M. Lewenstein, A. Sen(De), U. Sen, and J. Wehr, Classical spin models with broken symmetry: Random-field-induced order and persistence of spontaneous magnetization in the presence of a random field, Phys. Rev. B **90**, 174408 (2014).

[61] V. Grinenko, D. Das, R. Gupta, B. Zinkl, N. Kikugawa, Y. Maeno, C. W. Hicks, H.-H. Klauss, M. Sigrist, and R. Khasanov, Unsplit superconducting and time reversal symmetry breaking transitions in Sr_2RuO_4 under hydrostatic pressure and disorder, Nat. Commun. **12**, 3920 (2021).

[62] L. R. Testardi, Structural instability and superconductivity in A-15 compounds, Rev. Mod. Phys. **47**, 637 (1975).

[63] R. M. Fernandes and A. J. Millis, Nematicity as a Probe of Superconducting Pairing in Iron-Based Superconductors, Phys. Rev. Lett. **111**, 127001 (2013).

[64] M. Li, W. Cui, M. S. Dresselhaus, and G. Chen, Canonical quantization of crystal dislocation and electron-dislocation scattering in an isotropic medium, New J. Phys. **19**, 013033 (2017).

[65] M. Li, Z. Ding, Q. Meng, J. Zhou, Y. Zhu, H. Liu, M. S. Dresselhaus, and G. Chen, Nonperturbative quantum nature of the dislocation-phonon interaction, Nano Lett. **17**, 1587 (2017).

[66] G. Grimwall, *Thermophysical Properties of Materials* (North-Holland, Amsterdam, 1999).

[67] S. Hameed, D. Pelc, Z. W. Anderson, A. Klein, R. J. Spieker, M. Lukas, Y. Liu, M. J. Krogstad, R. Osborn, C. Leighton, R. M. Fernandes, and M. Greven, Ferroelectric quantum criticality and enhanced superconductivity in plastically deformed strontium titanate, arXiv:2005.00514.